
Hodge-Aware Learning on Simplicial Complexes

Anonymous Author(s)

Affiliation

Address

email

Abstract

1 Neural networks on simplicial complexes (SCs) can learn from data residing on
2 simplices such as nodes, edges, triangles, etc. However, existing works often
3 overlook the Hodge theory that decomposes simplicial data into three orthogonal
4 characteristic subspaces, such as the identifiable gradient, curl and harmonic com-
5 ponents of edge flows. In this paper, we aim to incorporate this data inductive bias
6 into learning on SCs. Particularly, we present a general convolutional architecture
7 which respects the three key principles of uncoupling the lower and upper sim-
8 plicial adjacencies, accounting for the inter-simplicial couplings, and performing
9 higher-order convolutions. To understand these principles, we first use Dirichlet
10 energy minimizations on SCs to interpret their effects on mitigating the simplicial
11 oversmoothing. Then, through the lens of spectral simplicial theory, we show the
12 three principles promote the Hodge-aware learning of this architecture, in the sense
13 that the three Hodge subspaces are invariant under its learnable functions and the
14 learning in two nontrivial subspaces are independent and expressive. To further
15 investigate the learning ability of this architecture, we also study it is stable against
16 small perturbations on simplicial connections. Finally, we experimentally validate
17 the three principles by comparing with methods that either violate or do not respect
18 them. Overall, this paper bridges learning on SCs with the Hodge decomposition,
19 highlighting its importance for rational and effective learning from simplicial data.

20 1 Introduction

21 It is not uncommon to have polyadic interactions in such as friendship networks [1], collaboration
22 networks [2], gene regulatory networks [3], etc [4-6]. To remedy the pitfall that graphs are limited to
23 model pairwise interactions between data entites on nodes, simplicial complexes (SCs) have become
24 popular among others [7]. A SC can be informally viewed as an extension of a graph, which is the
25 simplest SC, by including, not limited to, some triangles over the edge set. SCs like graphs have
26 algebraic representations – the Hodge Laplacians, an extension of graph Laplacians [8, 9]. Moreover,
27 besides node-wise data, SCs can support data on general simplices, e.g., flow-type data, e.g., water
28 flows [10], traffic flows [11], information flows [12], etc., naturally arise as data on edges, and data
29 related to three parties, e.g., triadic collaborations [2], can be defined on triangles in a SC.

30 Thus, existing works have built NNs on SCs to learn from such simplicial data, to name a few,
31 [13-19]. In analogous to graph neural networks (GNNs) learning from node data relying on the
32 adjacency between nodes, the idea behind these works is to rely on the relations between simplices.
33 Such relations can be twofold: first, two simplices can be lower and upper adjacent to each other,
34 such as an edge can be (lower) adjacent to another edge via a common node, and can also be (upper)
35 adjacent to others by sharing a common triangle; and second, there exist the inter-simplicial couplings
36 (or simplicial incidences) such that a node can induce data on its incident edge and a triangle can
37 cause data on its three edges, or the other way around. Along with this idea, [15, 16, 19] proposed
38 convolutional-type NNs by applying the simplicial adjacencies, [14, 20] included also inter-simplicial
39 couplings, and [17, 21] generalized the graph message-passing [22] to SCs based on both relations.

40 However, these works often solely focus on the simplicial structures, overlooking *the Hodge decom-*
41 *position* [23], which gives three orthogonal subspaces that uniquely characterize the simplicial data.
42 An edge flow can be decomposed into three distinct parts: a curl-free part induced by some node
43 data, a divergence-free (div-free) part that follows flow conservation (in-flows equal to out-flows at
44 nodes), and a harmonic part that is both div- and curl-free. Meanwhile, real-world simplicial data
45 often presents properties to be in certain subspaces but not others, or its components carry physical
46 usefulness, e.g., statistical ranking, exchange market [24], traffic networks [11], brain networks [12],
47 game theory [25], etc. Thus, intuitively, as an example, a Hodge-biased learner should not, at least not
48 primarily, learn in the div-free space if the edge flow is curl-free. If the learning function preserves the
49 subspaces and operates independently in three subspaces, the learning space is substantially shrunk.
50 This in fact provides an important inductive bias allowing for rational and effective learning on SCs.

51 Motivated by this, in this paper, we present the general convolutional learning on SCs, SCCNN, which
52 respects three key principles of uncoupling the lower and upper simplicial adjacencies, accounting
53 for the inter-simplicial couplings, and performing higher-order convolutions. Unlike existing convo-
54 lutional methods [14-16], which either lack theoretical insights or only discuss their architectural
55 differences in the simplicial domain, we focus on providing a theoretical analysis of these three
56 principles from both the perspectives of simplicial and simplicial data, specifically Hodge theory.
57 This offers deeper and unique insights when compared to the more closely related works [19, 17].

58 **Main contributions.** In Section 3.2, we first use Dirichlet energy minimizations on SCs to understand
59 how uncoupling the lower and upper adjacencies in Hodge Laplacians and the inter-simplicial
60 couplings can mitigate the oversmoothing inherited from generalizing GCN to SCs. Under the help
61 of spectral simplicial theory [26-28], in Section 4, we characterize the spectral behavior of SCCNN
62 and its expressive power. We show SCCNN performs independent and expressive learning in the
63 three subspaces of the Hodge decomposition, which are invariant under its learning operators. This
64 Hodge-awareness (or Hodge-aided bias) allows for effective and rational learning on SCs compared
65 to MLP or simplicial message-passing [17]. In Section 5, we also prove it is stable against small
66 perturbations on the strengths of simplicial connections, and show how three principles can affect the
67 stability. Lastly, we validate our findings on different simplicial tasks, including recovering foreign
68 currency exchange (forex) rates, predicting triadic and tetradic collaborations, and trajectories.

69 2 Background

70 **Simplicial complex and simplicial adjacencies.** A k -simplex s^k is a subset of $\mathcal{V} = \{1, \dots, n_0\}$
71 with cardinality $k + 1$. A *face* of s^k is a subset with cardinality k . A *coface* of s^k is a $(k + 1)$ -
72 simplex that has s^k as a face. Nodes, edges and (filled) triangles are geometric realizations of 0-
73 1- and 2-simplices. A SC \mathcal{S} of order K is a collection of k -simplices, $k = 0, \dots, K$, with the
74 *inclusion* property: $s^{k-1} \in \mathcal{S}$ if $s^{k-1} \subset s^k$ for $s^k \in \mathcal{S}$. A graph is a SC of order one and by
75 taking into account some triangles, we obtain a SC of order two. We collect all k -simplices of \mathcal{S}
76 in set $\mathcal{S}^k = \{s_i^k\}_{i=1, \dots, n_k}$ with $n_k = |\mathcal{S}^k|$, i.e., $\mathcal{S} = \cup_{k=0}^K \mathcal{S}^k$. For s^k , We say a k -simplex is *lower*
77 (*upper*) *adjacent* to s^k if they share a common face (coface). For computations, an *orientation* of a
78 simplex is chosen as an ordering of its vertices (a node has a trivial orientation). Here we consider
79 the lexicographical ordering $s^k = [1, \dots, k + 1]$, e.g., a triangle $s^2 = \{i, j, k\}$ is oriented as $[i, j, k]$.

80 **Algebraic representation.** Incidence matrix \mathbf{B}_k describes the relations between $(k - 1)$ - (i.e., faces)
81 and k -simplices, e.g., \mathbf{B}_1 is the node-to-edge incidence matrix and \mathbf{B}_2 edge-to-triangle. We have
82 $\mathbf{B}_k \mathbf{B}_{k+1} = \mathbf{0}$ by definition [9]. The k -Hodge Laplacian is $\mathbf{L}_k = \mathbf{B}_k^\top \mathbf{B}_k + \mathbf{B}_{k+1} \mathbf{B}_{k+1}^\top$ with the
83 *lower Laplacian* $\mathbf{L}_{k,d} = \mathbf{B}_k^\top \mathbf{B}_k$ and the *upper Laplacian* $\mathbf{L}_{k,u} = \mathbf{B}_{k+1} \mathbf{B}_{k+1}^\top$. We have a set of
84 $\mathbf{L}_k, k = 1, \dots, K - 1$ in a SC of order K with the graph Laplacian $\mathbf{L}_0 = \mathbf{B}_1 \mathbf{B}_1^\top$, and $\mathbf{L}_K = \mathbf{B}_K^\top \mathbf{B}_K$.
85 Note that $\mathbf{L}_{k,d}$ and $\mathbf{L}_{k,u}$ encode the lower and upper adjacencies of k -simplices. For example, for
86 $k = 1$, they encode the edge-to-edge adjacencies through nodes and triangles, respectively.

87 **Simplicial data.** A k -simplicial data (or k -signal) $\mathbf{x}_k \in \mathbb{R}^{n_k}$ is defined by an *alternating* map f_k
88 which assigns a real value to a simplex, and restricts that if the orientation of a simplex is anti-aligned
89 with the reference orientation, then the sign of the signal value will be changed [9].

90 **Incidence matrices as derivative operators on SCs.** We can measure how a k -signal \mathbf{x}_k varies w.r.t.
91 the faces and cofaces of k -simplices by applying $\mathbf{B}_k \mathbf{x}_k$ and $\mathbf{B}_{k+1}^\top \mathbf{x}_k$ [29]. For a node signal \mathbf{x}_0 , $\mathbf{B}_1^\top \mathbf{x}_0$
92 computes its *gradient* as the difference between adjacent nodes. Thus, a constant \mathbf{x}_0 has zero gradient.
93 For an edge flow \mathbf{x}_1 , $[\mathbf{B}_1 \mathbf{x}_1]_j = \sum_{i < j} [\mathbf{x}_1]_{[i,j]} - \sum_{j < k} [\mathbf{x}_1]_{[j,k]}$ computes its *divergence*, which is the

94 difference between the in-flow and the out-flow at node j , and $[\mathbf{B}_2^\top \mathbf{x}_1]_t = [\mathbf{x}_1]_{[i,j]} - [\mathbf{x}_1]_{[i,k]} + [\mathbf{x}_1]_{[j,k]}$
 95 computes the *curl* of \mathbf{x}_1 , which is the net-flow circulation in triangle $t = [i, j, k]$.

96 **Theorem 1** (Hodge decomposition [23, 9]). *The k -simplicial data space admits an orthogonal direct*
 97 *sum decomposition $\mathbb{R}^{n_k} = \text{im}(\mathbf{B}_k^\top) \oplus \text{ker}(\mathbf{L}_k) \oplus \text{im}(\mathbf{B}_{k+1})$. Moreover, we have $\text{ker}(\mathbf{B}_{k+1}^\top) =$*
 98 *$\text{im}(\mathbf{B}_k^\top) \oplus \text{ker}(\mathbf{L}_k)$ and $\text{ker}(\mathbf{B}_k) = \text{ker}(\mathbf{L}_k) \oplus \text{im}(\mathbf{B}_{k+1})$.*

99 In the node space, this is trivial as $\mathbb{R}^{n_0} = \text{ker}(\mathbf{L}_0) \oplus \text{im}(\mathbf{B}_1)$ where the kernel of \mathbf{L}_0 contains constant
 100 node data and the image of \mathbf{B}_1 contains nonconstant data. In the edge case, three subspaces carry
 101 more tangible meaning: the *gradient space* $\text{im}(\mathbf{B}_1^\top)$ collects edge flows as the gradient of some node
 102 signal, which are *curl-free*; the *curl space* $\text{im}(\mathbf{B}_2)$ consists of flows cycling around triangles, which
 103 are *div-free*; and flows in the *harmonic space* $\text{ker}(\mathbf{L}_1)$ are both div- and curl-free. In this paper, we
 104 inherit the names of three edge subspaces to general k -simplices. This theorem states that any \mathbf{x}_k can
 105 be uniquely expressed as $\mathbf{x}_k = \mathbf{x}_{k,G} + \mathbf{x}_{k,H} + \mathbf{x}_{k,C}$ with gradient part $\mathbf{x}_{k,G} = \mathbf{B}_k^\top \mathbf{x}_{k-1}$, curl part
 106 $\mathbf{x}_{k,C} = \mathbf{B}_{k+1} \mathbf{x}_{k+1}$, for some $\mathbf{x}_{k\pm 1}$, and harmonic part following $\mathbf{L}_k \mathbf{x}_{k,H} = \mathbf{0}$.

107 3 Simplicial Complex CNNs

108 We start by introducing the general convolutional architecture on SCs, followed by its properties, then
 109 we discuss its components from an energy minimizations perspective. We refer to [Appendix B](#) for
 110 some illustrations. In a SC, a SCCNN at layer l computes the k -output \mathbf{x}_k^l with \mathbf{x}_{k-1}^{l-1} , \mathbf{x}_k^{l-1} and \mathbf{x}_{k+1}^{l-1}
 111 as inputs, i.e., a map $\text{SCCNN}_k^l : \{\mathbf{x}_{k-1}^{l-1}, \mathbf{x}_k^{l-1}, \mathbf{x}_{k+1}^{l-1}\} \rightarrow \mathbf{x}_k^l$, for all k . It admits a detailed form

$$\mathbf{x}_k^l = \sigma(\mathbf{H}_{k,d}^l \mathbf{x}_{k,d}^{l-1} + \mathbf{H}_k^l \mathbf{x}_k^{l-1} + \mathbf{H}_{k,u}^l \mathbf{x}_{k,u}^{l-1}), \text{ with } \mathbf{H}_k^l = \sum_{t=0}^{T_d} w_{k,d,t}^l \mathbf{L}_{k,d}^t + \sum_{t=0}^{T_u} w_{k,u,t}^l \mathbf{L}_{k,u}^t. \quad (1)$$

112 1) Previous output \mathbf{x}_k^{l-1} is passed to a simplicial convolution filter (SCF [30]) \mathbf{H}_k^l of orders T_d, T_u ,
 113 which performs a linear combination of the data from up to T_d -hop lower-adjacent and T_u -hop
 114 upper-adjacent simplices, weighted by two sets of learnable weights $\{w_{k,d,t}^l\}, \{w_{k,u,t}^l\}$.

115 2) $\mathbf{x}_{k,d}^{l-1} = \mathbf{B}_k^\top \mathbf{x}_{k-1}^{l-1}$ and $\mathbf{x}_{k,u}^{l-1} = \mathbf{B}_{k+1} \mathbf{x}_{k+1}^{l-1}$ are the lower and upper projections from $(k \pm 1)$ -
 116 simplices via incidence relations, respectively. Then, $\mathbf{x}_{k,d}^{l-1}$ is passed to a lower SCF $\mathbf{H}_{k,d}^l :=$
 117 $\sum_{t=0}^{T_d} w_{k,d,t}^l \mathbf{L}_{k,d}^t$, and the upper projection $\mathbf{x}_{k,u}^{l-1}$ is passed to an upper SCF $\mathbf{H}_{k,u}^l := \sum_{t=0}^{T_u} w_{k,u,t}^l \mathbf{L}_{k,u}^t$.
 118 Lastly, the sum of the three SCF outputs is passed to an elementwise nonlinearity $\sigma(\cdot)$.

119 This architecture subsumes the methods in [14–16, 19, 18, 20]. Particularly, we emphasize on the key
 120 three principles. 1) Uncouple the lower and upper Laplacians: this leads to an independent treatment
 121 of the lower and upper adjacencies, achieved by using two sets of learnable weights; 2) Account for
 122 the inter-simplicial couplings: $\mathbf{x}_{k,d}$ and $\mathbf{x}_{k,u}$ carry the nontrivial information contained in the faces
 123 and cofaces (by [Theorem 1](#)); and 3) Perform higher-order convolutions: considering $T_d, T_u \geq 1$ in
 124 SCFs which leads to a multi-hop receptive field on SCs. In short, SCCNN propagates information
 125 across SCs based on two simplicial adjacencies and two incidences in a multi-hop fashion.

126 3.1 Properties

127 **Simplicial locality.** SCFs admit an intra-simplicial locality: $\mathbf{H}_k \mathbf{x}_k$ is localized in T_d -hop lower and
 128 T_u -hop upper k -simplicial neighborhoods [30]. A SCCNN preserves such locality as $\sigma(\cdot)$ does not
 129 alter the information locality. It also admits the inter-simplicial locality between k - and $(k \pm 1)$ -
 130 simplices, which extends to simplices of orders $k \pm 2$ if $L \geq 2$ because $\mathbf{B}_k \sigma(\mathbf{B}_{k+1}) \neq \mathbf{0}$ [31].
 131 Moreover, the two localities are coupled in a multi-hop way through SCFs such that a node not only
 132 interacts with its incident edges and the triangles including it, but also those further hops away.

133 **Complexity.** A SCCNN layer has the parameter complexity of order $\mathcal{O}(T_d + T_u)$ and the computa-
 134 tional complexity $\mathcal{O}(k(n_k + n_{k+1}) + n_k m_k (T_d + T_u))$, linear to the simplex dimensions, where m_k
 135 is the maximum of the number of neighbors for k -simplices.

136 **Equivariance.** SCCNNs are permutation-equivariant, which allows us to list simplices in any order,
 137 and orintation-equivariant if $\sigma(\cdot)$ is odd, which gives us the freedom to choose reference orientations.
 138 In [Appendix B.3](#), we provide formal discussions on such equivariances and why permutations form a
 139 symmetry group of a SC and orientation changes are symmetries of data space but not SCs.

140 3.2 A perspective of SCCNN from Dirichlet energy minimization on SCs

141 **Definition 2.** The *Dirichlet energy* of \mathbf{x}_k is $D(\mathbf{x}_k) = D_d(\mathbf{x}_k) + D_u(\mathbf{x}_k) := \|\mathbf{B}_k \mathbf{x}_k\|_2^2 + \|\mathbf{B}_{k+1}^\top \mathbf{x}_k\|_2^2$.

142 For node signals, $D(\mathbf{x}_0) = \|\mathbf{B}_1^\top \mathbf{x}_0\|_2^2 = \sum_i \sum_j \|x_{0,i} - x_{0,j}\|^2$ is a ℓ_2 -norm of the *gradient* of \mathbf{x}_0 .
 143 For edge flows, $D(\mathbf{x}_1)$ is the sum of the total divergence and curl, which measure the flow variations
 144 w.r.t. nodes and triangles, respectively. In general, $D(\mathbf{x}_k)$ measures the lower and upper k -simplicial
 145 signal variations w.r.t. the faces ($D_d(\mathbf{x}_k)$) and cofaces ($D_u(\mathbf{x}_k)$). A k -signal \mathbf{x}_k with $D(\mathbf{x}_k) = 0$
 146 follows $\mathbf{L}_k \mathbf{x}_k = \mathbf{0}$, called *harmonic*, e.g., a constant node signal and a div- and curl-free edge flow.

147 **Simplicial shifting as Hodge Laplacian smoothing.** [14, 20] considered \mathbf{H}_k as a weighted variant
 148 of $\mathbf{I} - \mathbf{L}_k$, generalizing the GCN layer [32]. This simplicial shifting step is necessarily a Hodge
 149 Laplacian smoothing [31]. Given an initial \mathbf{x}_k^0 , we consider the Dirichlet energy minimization:

$$\min_{\mathbf{x}_k} \|\mathbf{B}_k \mathbf{x}_k\|_2^2 + \gamma \|\mathbf{B}_{k+1}^\top \mathbf{x}_k\|_2^2, \gamma > 0, \text{ gradient descent: } \mathbf{x}_{k,\text{gd}}^{l+1} = (\mathbf{I} - \eta \mathbf{L}_{k,\text{d}} - \eta \gamma \mathbf{L}_{k,\text{u}}) \mathbf{x}_k^l \quad (2)$$

150 with step size $\eta > 0$. The simplicial shifting $\mathbf{x}_k^{l+1} = w_0(\mathbf{I} - \mathbf{L}_k) \mathbf{x}_k^l$ is a gradient descent with
 151 $\eta = \gamma = 1$ and weighted by w_0 , then followed by nonlinearity. A minimizer of Eq. (2) with $\gamma = 1$ is
 152 in the harmonic space $\ker(\mathbf{L}_k)$. Thus, an NN composed of simplicial shifting layers may lead to an
 153 output with exponentially decreasing Dirichlet energy as it deepens, i.e., *simplicial oversmoothing*.

154 **Proposition 3.** If $w_0^2 \|\mathbf{I} - \mathbf{L}_k\|_2^2 < 1$, $D(\mathbf{x}_k^{l+1})$ in a simplicial shifting exponentially converges to 0.

155 This generalizes the oversmoothing of GCN and its variants [33–35]. However, when uncoupling
 156 the lower and upper parts of \mathbf{L}_k in this shifting, associated with $\gamma \neq 1$, the decrease of $D(\mathbf{x}_k)$ can
 157 slow down or cease because the objective instead looks for a solution primarily in either $\ker(\mathbf{B}_k)$
 158 (for $\gamma \ll 1$) or $\ker(\mathbf{B}_{k+1}^\top)$ (for $\gamma \gg 1$), not necessarily in $\ker(\mathbf{L}_k)$, as we show in Section 6.

159 **Inter-simplicial couplings as sources.** Given some nontrivial \mathbf{x}_{k-1} and \mathbf{x}_{k+1} , we consider

$$\min_{\mathbf{x}_k} \|\mathbf{B}_k \mathbf{x}_k - \mathbf{x}_{k-1}\|_2^2 + \|\mathbf{B}_{k+1}^\top \mathbf{x}_k - \mathbf{x}_{k+1}\|_2^2, \quad (3)$$

160 which has a gradient descent $\mathbf{x}_{k,\text{gd}}^{l+1} = (\mathbf{I} - \eta \mathbf{L}_k) \mathbf{x}_k^l + \eta(\mathbf{x}_{k,\text{d}} + \mathbf{x}_{k,\text{u}})$. It resembles the whole layer
 161 in [14, 20], $\mathbf{x}_k^{l+1} = w_0(\mathbf{I} - \mathbf{L}_k) \mathbf{x}_k^l + w_1 \mathbf{x}_{k,\text{d}} + w_2 \mathbf{x}_{k,\text{u}}$ with some weights, followed by nonlinearity.
 162 We have $D(\mathbf{x}_k^{l+1}) \leq w_0^2 \|\mathbf{I} - \mathbf{L}_k\|_2^2 D(\mathbf{x}_k^l) + w_1^2 \lambda_{\max}(\mathbf{L}_{k,\text{d}}) \|\mathbf{x}_{k,\text{d}}\|_2^2 + w_2^2 \lambda_{\max}(\mathbf{L}_{k,\text{u}}) \|\mathbf{x}_{k,\text{u}}\|_2^2$, by
 163 triangle inequality. The projections here act as energy sources, and also the objective looks for an
 164 \mathbf{x}_k in the images of \mathbf{B}_{k+1} and \mathbf{B}_k^\top , instead of $\ker(\mathbf{L}_k)$ when \mathbf{x}_{k-1} and \mathbf{x}_{k+1} are not trivial. Thus,
 165 inter-simplicial couplings can potentially mitigate the oversmoothing as well.

166 Here we show simply generalizing GCN will inherit its oversmoothing to SCs. However, both the
 167 separation of the lower and upper Laplacians and inter-simplicial couplings could potentially mitigate
 168 this oversmoothing. We here considered a Dirichlet energy minimization perspective. They can also
 169 be explained by means of diffusion process on SCs [36]. We refer to Appendix B.4 for this.

170 4 From convolutional to Hodge-aware

171 In this section, we show how SCCNN, guided by the three principles, performs *the Hodge-aware*
 172 *learning*, allowing for rational and effective learning on SCs while remaining expressive. To ease the
 173 exposition, we first provide a more fine-grained spectral view on how SCCNN learns from simplicial
 174 data of different variations in the three subspaces based on the simplicial spectral theory [27, 26, 30].
 175 Then, we characterize its expressive power and discuss its Hodge-awareness.

176 **Definition 4** ([27]). The simplicial Fourier transform (SFT) of \mathbf{x}_k is $\tilde{\mathbf{x}}_k = \mathbf{U}_k^\top \mathbf{x}_k$ where the Fourier
 177 basis \mathbf{U}_k can be found as the eigenbasis of \mathbf{L}_k and the eigenvalues are *simplicial frequencies*.

178 **Proposition 5** ([26]). *The SFT basis can be found as $\mathbf{U}_k = [\mathbf{U}_{k,\text{H}} \ \mathbf{U}_{k,\text{G}} \ \mathbf{U}_{k,\text{C}}]$ where 1) the zero*
 179 *eigenspace $\mathbf{U}_{k,\text{H}}$ of \mathbf{L}_k spans $\ker(\mathbf{L}_k)$, and an eigenvalue $\lambda_{k,\text{H}} = 0$ is a harmonic frequency; 2) the*
 180 *nonzero eigenspace $\mathbf{U}_{k,\text{G}}$ of $\mathbf{L}_{k,\text{d}}$ spans $\text{im}(\mathbf{B}_k^\top)$, and an eigenvalue $\lambda_{k,\text{G}}$ is a gradient frequency,*
 181 *measuring the lower variation $D_d(\mathbf{u}_{k,\text{G}})$; 3) the nonzero eigenspace $\mathbf{U}_{k,\text{C}}$ of $\mathbf{L}_{k,\text{u}}$ spans $\text{im}(\mathbf{B}_{k+1})$,*
 182 *and an eigenvalue $\lambda_{k,\text{C}}$ is a curl frequency, measuring the upper variation $D_u(\mathbf{u}_{k,\text{C}})$.*

183 Thus, the SFT of \mathbf{x}_k can be found as $\tilde{\mathbf{x}}_k = [\tilde{\mathbf{x}}_{k,\text{H}}^\top, \tilde{\mathbf{x}}_{k,\text{G}}^\top, \tilde{\mathbf{x}}_{k,\text{C}}^\top]^\top$, where each component is the
 184 intensity of \mathbf{x}_k at a simplicial frequency. Consider $\mathbf{y}_k = \mathbf{H}_{k,\text{d}} \mathbf{x}_{k,\text{d}} + \mathbf{H}_k \mathbf{x}_k + \mathbf{H}_{k,\text{u}} \mathbf{x}_{k,\text{u}}$ in a SCCNN
 185 layer. Multiplying on both sides by \mathbf{U}_k , we then have the SFT $\tilde{\mathbf{y}}$ as

$$\begin{cases} \tilde{\mathbf{y}}_{k,\text{H}} = \tilde{\mathbf{h}}_{k,\text{H}} \odot \tilde{\mathbf{x}}_{k,\text{H}}, \\ \tilde{\mathbf{y}}_{k,\text{G}} = \tilde{\mathbf{h}}_{k,\text{d}} \odot \tilde{\mathbf{x}}_{k,\text{d}} + \tilde{\mathbf{h}}_{k,\text{G}} \odot \tilde{\mathbf{x}}_{k,\text{G}}, \\ \tilde{\mathbf{y}}_{k,\text{C}} = \tilde{\mathbf{h}}_{k,\text{C}} \odot \tilde{\mathbf{x}}_{k,\text{C}} + \tilde{\mathbf{h}}_{k,\text{u}} \odot \tilde{\mathbf{x}}_{k,\text{u}}, \end{cases} \quad \text{where} \quad \begin{cases} \tilde{\mathbf{h}}_{k,\text{H}} = (w_{k,\text{d},0} + w_{k,\text{u},0}) \mathbf{1}, \\ \tilde{\mathbf{h}}_{k,\text{G}} = \sum_{t=0}^{T_d} w_{k,\text{d},t} \lambda_{k,\text{G}}^{\odot t} + w_{k,\text{u},0} \mathbf{1}, \\ \tilde{\mathbf{h}}_{k,\text{C}} = \sum_{t=0}^{T_u} w_{k,\text{u},t} \lambda_{k,\text{C}}^{\odot t} + w_{k,\text{d},0} \mathbf{1}, \end{cases} \quad (4)$$

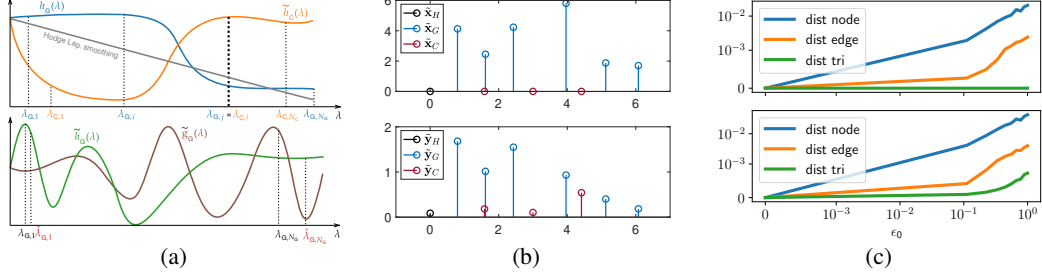


Figure 1: (a) (*top*): Independent gradient and curl learning responses. (*bottom*): Stability-selectivity tradeoff of SCFs where \tilde{h}_G has better stability but smaller selectivity than \tilde{h}_C . (b) Information spillage of nonlinearity. (c) The distance between the perturbed outputs and true when node adjacencies are perturbed. (*top*): $L = 1$, triangle output remains clean. (*bottom*): $L = 2$, triangle output is perturbed.

186 is the frequency response of \mathbf{H}_k as $\tilde{\mathbf{h}}_k = \text{diag}(\mathbf{U}_k^\top \mathbf{H}_k \mathbf{U}_k)$ [30], and $\tilde{\mathbf{h}}_{k,d}$ and $\tilde{\mathbf{h}}_{k,u}$, the responses of
 187 $\mathbf{H}_{k,d}$ and $\mathbf{H}_{k,u}$, can be expressed accordingly. This spectral relation (4) shows how the learning of
 188 SCCNN is performed at frequencies in different subspaces. Specifically, the gradient SFT $\tilde{\mathbf{x}}_{k,G}$ is
 189 learned by a gradient response $\tilde{\mathbf{h}}_{k,G}$, which is independent of the curl response $\tilde{\mathbf{h}}_{k,C}$ learning the curl
 190 SFT $\tilde{\mathbf{x}}_{k,C}$, and they only coincide at the trivial harmonic frequency, as shown in Fig. 1a. Likewise,
 191 the lower and upper projections are independently learned by $\tilde{\mathbf{h}}_{k,d}$ and $\tilde{\mathbf{h}}_{k,u}$, respectively.

192 The nonlinearity induces the information spillage that one type of spectra could be spread over other
 193 types. That is, $\sigma(\tilde{\mathbf{y}}_{k,G})$ could contain information in harmonic or curl subspaces, as illustrated in
 194 Fig. 1b. This is to increase the expressive power of SCCNN, which can be characterized as follows.

195 **Theorem 6.** A SCCNN layer with inputs $\mathbf{x}_{k,d}, \mathbf{x}_k, \mathbf{x}_{k,u}$ is at most expressive as an MLP layer
 196 $\sigma(\mathbf{G}'_{k,d}\mathbf{x}_{k,d} + \mathbf{G}_k\mathbf{x}_k + \mathbf{G}'_{k,u}\mathbf{x}_{k,u})$ with $\mathbf{G}_k = \mathbf{G}_{k,d} + \mathbf{G}_{k,u}$ where $\mathbf{G}_{k,d}$ and $\mathbf{G}_{k,u}$ are analytical
 197 matrix functions of $\mathbf{L}_{k,d}$ and $\mathbf{L}_{k,u}$, respectively, and $\mathbf{G}'_{k,d}$ and $\mathbf{G}'_{k,u}$ likewise. Moreover, this expres-
 198 sivity can be achieved when setting $T_d = T'_d = n_{k,G}$ and $T_u = T'_u = n_{k,C}$ in Eq. (1) with $n_{k,G}$ the
 199 number of distinct gradient frequencies and $n_{k,C}$ the number of distinct curl frequencies.

200 The proof follows from Cayley-Hamilton theorem [37]. This expressive power can be better under-
 201 stood spectrally. The gradient SFT of \mathbf{x}_k can be learned most expressively by an analytical function
 202 $g_{k,G}(\lambda)$, the eigenvalue of $\mathbf{G}_{k,d}$ at a gradient frequency. And the curl SFT of \mathbf{x}_k can be learned
 203 most expressively by another analytical function $g_{k,C}(\lambda)$, the eigenvalue of $\mathbf{G}_{k,u}$ at a curl frequency.
 204 These two functions only need to coincide at harmonic frequency $\lambda = 0$. The SFTs of lower and
 205 upper projections can be learned most expressively by two independent functions as well. Given this
 206 expressive power and Eq. (4) we show SCCNN performs the Hodge-aware learning as follows.

207 **Theorem 7.** A SCCNN is Hodge-aware in the sense that 1) three Hodge subspaces are *invariant* under
 208 the learnable SCF \mathbf{H}_k , i.e., $\mathbf{H}_k\mathbf{x} \in \text{im}(\mathbf{B}_k^\top)$ if $\mathbf{x} \in \text{im}(\mathbf{B}_k^\top)$, and likewise for $\text{im}(\mathbf{B}_{k+1})$, $\ker(\mathbf{L}_k)$;
 209 2) the gradient and curl spaces are invariant under the learnable lower SCF $\mathbf{H}_{k,d}$ and upper SCF
 210 $\mathbf{H}_{k,u}$, respectively; 3) the learning in the gradient and curl spaces are *independent and expressive*.

211 This theorem essentially shows SCCNN performs expressive learning independently in the gradient
 212 and curl subspaces from three inputs while preserving the three subspaces to be invariant w.r.t its
 213 learning functions. This allows for the **rational and effective learning** on SCs. On one hand, the
 214 invariance of subspaces under the learnable SCFs substantially shrinks the learning space and makes
 215 SCCNN effective, meanwhile, its expressive power is guaranteed by the independent expressive
 216 learners, together with the nonlinearity. Instead, the non-Hodge-aware learning, e.g., MLP or
 217 simplicial message-passing using MLP to aggregate and update [17], has a much larger learning space
 218 which requires more training data for accurate learning, as well as larger computational complexity.

219 On the other hand, simplicial data often presents (implicit or explicit) properties that Hodge subspaces
 220 can capture. For example, water flows, traffic flows, electric currents [29, 11] follow flow conservation
 221 (div-free, in $\ker(\mathbf{B}_1)$), or curl-free forex rates, as we show in Section 6, or the gradient component of
 222 pairwise comparison data gives consistent global ranking but others are unwanted [24]. SCCNN is
 223 able to capture these characteristics effectively, generating rational outputs due to the invariance of
 224 subspaces and independent learning in gradient and curl spaces. We illustrate a trivial example below.

225 *Example 8.* Suppose learning to remove non-div-free noise from some input for flow conservation.
 226 SCCNN can correctly do so because when a not-well-learned SCF, preserving the noise and useful

227 parts primarily in their own spaces, causes large loss, e.g., mse, the Hodge-awareness restricts it to
 228 suppress in the gradient space and preserve in others. This however can be difficult non-Hodge-aware
 229 learners, e.g., MLP or MPSN [17], especially when the amount of data is limited, because the
 230 non-div-free noise can be disguised as useful by their unbiased transformation into other spaces,
 231 and the useful parts could be transformed into noise space, generating irrational non-div-free output
 232 though the overall mse can be small. *Thus, simplicial data characteristics can be easily ignored by*
 233 *non-Hodge-aware learners when the invariance condition is not satisfied.*

234 **Comparison to others.** We here discuss some other existing learning methods on SCs to emphasize on
 235 the Hodge-awareness. [15] considered $\mathbf{H}_k = \sum_i w_i \mathbf{L}_k^i$ to perform convolutions without uncoupling
 236 the lower and upper parts of \mathbf{L}_k , which makes it *strictly less expressive* and non-Hodge-aware,
 237 because it cannot perform different learning at frequencies in both gradient and curl spaces, though
 238 deeper layers and higher orders can compensate its expressive at other frequencies. [16] applied
 239 \mathbf{H}_k with $T_d = T_u = 1$, which has a limited linear learning response. SCCNN returns the methods
 240 in [19, 38] when there is no inter-simplicial coupling needed. [14, 20] took the form of simplicial
 241 shifting by generalizing the GCN without uncoupling the two adjacencies, which is not-Hodge-aware.
 242 Spectrally, this gives a limited lower-pass linear spectral response, shown in Fig. 1a.

243 5 How robust are SCCNNs to domain perturbations?

244 In practice, a SCCNN is often built on a weighted SC to capture the strengths of simplicial adjacencies
 245 and incidences, with a same form as Eq. (1), except for that the Hodge Laplacians and the projection
 246 matrices are weighted, denoted as general operators $\mathbf{R}_{k,d}$, $\mathbf{R}_{k,u}$. These matrices are often defined
 247 following [29, 39, 40], e.g., [14, 20] considered a particular random walk formulation [41], or can
 248 be learned from data, e.g., via an attention method [42, 38]. Since SCCNN relies on the Hodge
 249 Laplacians and projection matrices, in this section, we address the question, *when these operators*
 250 *are perturbed, how accurate and robust are the outputs of a SCCNN?* This models the domain
 251 perturbations on the strengths of adjacent and incident relations such as a large weight is applied
 252 when two edges are weakly or not adjacent, or data on a node projects on an edge not incident to it.
 253 By quantifying this stability, we can explain the robust learning ability of SCCNN. We consider a
 254 relative perturbation model, also used to study the stability of CNNs [43-45] and GNNs [46-49].

255 Denote the perturbed lower and upper Laplacians as $\widehat{\mathbf{L}}_{k,d}$ and $\widehat{\mathbf{L}}_{k,u}$ by perturbations $\mathbf{E}_{k,d}$ and $\mathbf{E}_{k,u}$,
 256 and the lower and upper projections as $\widehat{\mathbf{R}}_{k,d}$ and $\widehat{\mathbf{R}}_{k,u}$ by perturbations $\mathbf{J}_{k,d}$ and $\mathbf{J}_{k,u}$, respectively.

257 **Definition 9** (Relative perturbation). Consider some perturbation matrix \mathbf{E} of an appropriate dimen-
 258 sion. For a symmetric matrix \mathbf{A} , its (relative) perturbed version is $\widehat{\mathbf{A}}(\mathbf{E}) = \mathbf{A} + \mathbf{E}\mathbf{A} + \mathbf{A}\mathbf{E}$. For a
 259 rectangular matrix \mathbf{B} , its (relative) perturbed version is $\widehat{\mathbf{B}}(\mathbf{E}) = \mathbf{B} + \mathbf{E}\mathbf{B}$.

260 This relative perturbation model, in contrast to an absolute one [47], quantifies perturbations w.r.t. the
 261 local simplicial topology in the sense that weaker connections in a SC are deviated by perturbations
 262 proportionally less than stronger connections. We further consider the integral Lipschitz property,
 263 extended from [47], to measure the variability of spectral response functions of \mathbf{H}_k .

264 **Definition 10.** A SCF \mathbf{H}_k is *integral Lipschitz* with constants $c_{k,d}, c_{k,u} \geq 0$ if the derivatives of
 265 response functions $\tilde{h}_{k,G}(\lambda)$ and $\tilde{h}_{k,C}(\lambda)$ follow that $|\lambda \tilde{h}'_{k,G}(\lambda)| \leq c_{k,d}$ and $|\lambda \tilde{h}'_{k,C}(\lambda)| \leq c_{k,u}$.

266 This property provides a stability-selectivity tradeoff of SCFs independently in gradient and curl
 267 frequencies. A spectral response can have both good selectivity and stability in small frequencies
 268 (a large $|\tilde{h}'_{k,\cdot}|$ for $\lambda \rightarrow 0$), while in large frequencies, it tends to be flat for better stability at the
 269 cost of selectivity (a small variability for large λ), as shown in Fig. 1a. As of the polynomial nature
 270 of responses, all SCFs of a SCCNN are integral Lipschitz. We also denote the integral Lipschitz
 271 constant for the lower SCFs $\mathbf{H}_{k,d}$ by $c_{k,d}$ and for the upper SCFs $\mathbf{H}_{k,u}$ by $c_{k,u}$. Given the following
 272 reasonable assumptions, we are ready to characterize the stability bound of a SCCNN.

273 **Assumption 11.** a) *The perturbations are small such that $\|\mathbf{E}_{k,d}\|_2 \leq \epsilon_{k,d}$, $\|\mathbf{J}_{k,d}\|_2 \leq \epsilon_{k,d}$, $\|\mathbf{E}_{k,u}\|_2 \leq$
 274 $\epsilon_{k,u}$ and $\|\mathbf{J}_{k,u}\|_2 \leq \epsilon_{k,u}$.* b) *The SCFs \mathbf{H}_k of a SCCNN have a normalized bounded frequency*
 275 *response (for simplicity, though unnecessary), likewise for $\mathbf{H}_{k,d}$ and $\mathbf{H}_{k,u}$.* c) *The lower and upper*
 276 *projections are finite $\|\mathbf{R}_{k,d}\|_2 \leq r_{k,d}$ and $\|\mathbf{R}_{k,u}\|_2 \leq r_{k,u}$.* d) *The nonlinearity $\sigma(\cdot)$ is c_σ -Lipschitz*
 277 *(e.g., relu, tanh, sigmoid).* e) *The initial input \mathbf{x}_k^0 , for all k , is finite, $\|\mathbf{x}_k^0\|_2 \leq [\beta]_k$.*

278 **Theorem 12.** *Let \mathbf{x}_k^L be the k -simplicial output of an L -layer SCCNN on a weighted SC. Let $\tilde{\mathbf{x}}_k^L$ be*
 279 *the output of the same SCCNN but on a relatively perturbed SC. Under Assumption 11, the Euclidean*

280 distance between the two outputs is finite and upper-bounded $\|\hat{\mathbf{x}}_k^L - \mathbf{x}_k^L\|_2 \leq [\mathbf{d}]_k$ where

$$\mathbf{d} = c_\sigma^L \sum_{l=1}^L \hat{\mathbf{Z}}^{l-1} \mathbf{T} \mathbf{Z}^{L-l} \boldsymbol{\beta}, \text{ with, e.g., } \mathbf{T} = \begin{bmatrix} t_0 & t_{0,u} & \\ t_{1,d} & t_1 & t_{1,u} \\ & t_{2,d} & t_2 \end{bmatrix} \mathbf{Z} = \begin{bmatrix} 1 & r_{0,u} & \\ r_{1,d} & 1 & r_{1,u} \\ & r_{2,d} & 1 \end{bmatrix}, \quad (5)$$

281 for $K = 2$, which are tridiagonal, and $\hat{\mathbf{Z}}$ is defined as \mathbf{Z} but with off-diagonal entries $\hat{r}_{k,d} =$
 282 $r_{k,d}(1 + \varepsilon_{k,d})$ and $\hat{r}_{k,u} = r_{k,u}(1 + \varepsilon_{k,u})$. Diagonal entries of \mathbf{T} are $t_k = c_{k,d} \Delta_{k,d} \varepsilon_{k,d} + c_{k,u} \Delta_{k,u} \varepsilon_{k,u}$,
 283 and off-diagonals are $t_{k,d} = r_{k,d} \varepsilon_{k,d} + c_{k,d} \Delta_{k,d} \varepsilon_{k,d} r_{k,d}$ and $t_{k,u} = r_{k,u} \varepsilon_{k,u} + c_{k,u} \Delta_{k,u} \varepsilon_{k,u} r_{k,u}$,
 284 where $\Delta_{k,d}$ captures the eigenvector misalignment between $\mathbf{L}_{k,d}$ and perturbation $\mathbf{E}_{k,d}$ with a factor
 285 $\sqrt{n_k}$, and likewise for $\Delta_{k,u}$.

286 This result bounds the outputs of a SCCNN on all simplicial levels, showing they are stable to
 287 small perturbations on the strengths of simplicial adjacencies and incidences. Specifically, we make
 288 two observations from the seemingly complicated expression. 1) The stability bound depends on
 289 i) the degree of perturbations including their magnitude ε and ε , and eigenspace misalignment Δ ,
 290 ii) the integral Lipschitz properties of SCFs, and iii) the degree of projections r . 2) The stability of
 291 k -output depends on factors of not only k -simplices, but also simplices of adjacent orders due to
 292 inter-simplicial couplings. When $L = 1$, node output bound d_0 depends on factors in the node space,
 293 as well as the edge space factored by the projection degree, and vice versa for edge output. As the
 294 layer deepens, this mutual dependence expands further. When $L = 2$, factors in the triangle space
 295 also affect the stability of node output d_0 , and vice versa for triangle output, as observed in [Fig. 1c](#).

296 More importantly, this stability provides practical implications for learning on SCs. While accounting
 297 for inter-simplicial couplings may be beneficial, it does not help with the stability of SCCNNs when
 298 the number of layers increases due to the mutual dependence between different outputs. Thus, to
 299 maintain the expressive power, higher-order SCFs can be used in exchange for shallow layers. This
 300 does not harm the stability because, first, the components of high-frequency can be spread over the
 301 low frequency due to the nonlinearity where the spectral responses are more selective without losing
 302 the stability; and second, higher-order SCFs are easier to be learned with smaller integral Lipschitz
 303 constants than lower-order ones, thus, better stability. The latter can be easily seen by comparing
 304 one-order and two-order cases. We also experimentally show this in [Fig. 4](#).

305 6 Experiments

306 **Synthetic.** We first illustrate the evolution of Dirichlet energies
 307 of outputs on nodes, edges and triangles of a SC of order two by
 308 numbers of simplicial shifting layers with $\sigma = \tanh$. The inputs
 309 on them are randomly sampled from $\mathcal{U}([-5, 5])$. [Fig. 2](#) shows
 310 simply generalizing GCN on SCs could lead to oversmoothing
 311 on simplices of all orders. However, uncoupling the lower and
 312 upper parts of \mathbf{L}_1 by setting, e.g., $\gamma = 2$ could mitigate the
 313 oversmoothing on edges. Lastly, the inter-simplicial coupling
 314 could almost prevent the oversmoothing.

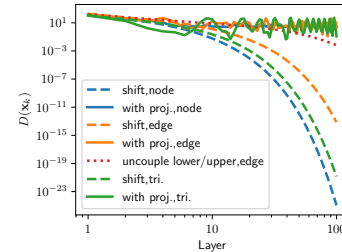


Figure 2

315 **Foreign currency exchange.** In forex problems, for any currencies i, j, k , the *arbitray-free* condition
 316 of a fair market reads as $r^{i/j} r^{j/k} = r^{i/k}$ with the exchange rate $r^{i/j}$ between i and j . That is, the
 317 exchange path $i \rightarrow j \rightarrow k$ provides no profit or loss over a direct exchange $i \rightarrow k$. By modeling the
 318 forex as a SC of order two and the exchange rates as edge flows $[\mathbf{x}_1]_{[i,j]} = \log(r^{i/j})$, this condition
 319 translates as \mathbf{x}_1 is curl-free, i.e., $[\mathbf{x}_1]_{[i,j]} + [\mathbf{x}_1]_{[j,k]} - [\mathbf{x}_1]_{[i,k]} = 0$ in any triangle $[i, j, k]$ [\[24\]](#). Here
 320 we consider a real-world forex market from [\[50\]](#) at three timestamps, which contains certain degree
 321 of arbitrage. We artificially added some random noise and “curl noise” (only in the curl space) to
 322 this market, in which we aim to recover the forex rates. We also randomly masked 50% of the rates,
 323 where we aim to interpolate the market such that it is arbitrage-free. Three settings create three types
 324 of learning needs. To evaluate the performance, we measure both normalized mse and total arbitrage
 325 (total curl), both equally important for the goal of *creating a fair market by small price fluctuations*.

326 From [Table 1](#), we make the following observations. 1) MPSN [\[17\]](#) fails at this task: although it
 327 can reduce nmse, it outputs unfair rates with large arbitrage, which is against the forex principle,
 328 because it is not Hodge-aware, unable to capture the arbitrage-free property with small amount of
 329 data. 2) SNN [\[15\]](#) fails too: as discussed in [Section 4](#) it restricts the gradient and curl spaces to be
 330 always learned in the same fashion, unable to meet the need of disjoint learning of this task in two

Table 1: Forex results (nmse|total arbitrage).

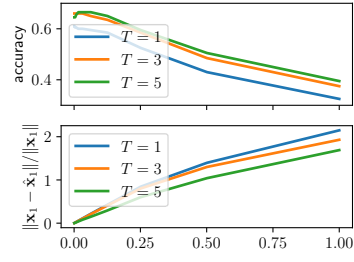
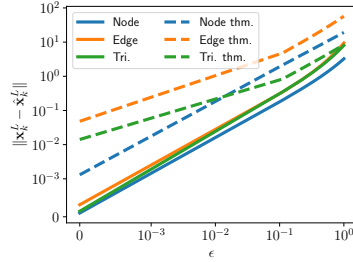
Methods	Random Noise		Curl Noise		Interpolation	
Input	.119±.004	29.19±.874	.552±.027	122.4±5.90	.717±.030	106.4±.902
Baseline	.036±.005	2.29±.079	.050±.002	11.12±.537	.534±.043	9.67±.082
SNN [15]	.110±.005	23.24±1.03	.446±.017	86.95±2.20	.702±.033	104.74±1.04
PSNN [16]	.008±.001	.984±.170	.000±.000	.000±.000	.009±.001	1.13±.329
MPSN [17]	.039±.004	7.74±0.88	.076±.012	14.92±2.49	.117±.063	23.15±11.7
SCCNN, id	.027±.005	.000±.000	.000±.000	.000±.000	.265±.036	.000±.000
SCCNN, tanh	.002±.000	.325±.082	.000±.000	.003±.003	.003±.002	.279±.151

Table 2: Simplex prediction.

Methods	2-simplex	3-simplex
Mean [2]	62.8±2.7	63.6±1.6
MLP	68.5±1.6	69.0±2.2
GNN [51]	93.9±1.0	96.6±0.5
SNN [15]	92.0±1.8	95.1±1.2
PSNN [16]	95.6±1.3	98.1±0.5
SCNN [19]	96.5±1.5	98.3±0.4
Bunch [14]	98.3±0.5	98.5±0.5
MPSN [17]	98.1±0.5	99.2±0.3
SCCNN	98.7±0.5	99.4±0.3

Table 3: Ablation study.

Missing	2-Simplex	Param.
—	98.7±0.5	$L = 2$
Edge-to-Node	93.9±1.0	$L = 5$
Node-to-Node	98.7±0.4	$L = 4$
Edge-to-Edge	98.5±1.0	$L = 3$
Node-to-Edge	98.8±0.3	$L = 4$
Node input	98.2±0.5	$T = 4$
Edge input	98.1±0.4	$T = 3$

Figure 3: Stability bound. Figure 4: Stability as T increases.

spaces. 3) PSNN [16] can reconstruct relatively fair forex rates with small nmse. In the curl noise case, the reconstruction is perfect, while in the other two cases, the nmse and arbitrage are three times larger than SCCNN due to its limited linear learning responses. 4) SCCNN performs the best in both reducing the total error and the total arbitrage. We also notice that with $\sigma = \text{id}$, the arbitrage-free rule is fully learned by SCCNN. However, it has relatively larger errors in the random and interpolation cases due to its limited linear expressive power. With $\sigma = \text{tanh}$, SCCNN can tackle these more challenging cases, finding a good compromise between overall error and data characteristics.

Simplex Prediction. We then test SCCNN on simplex prediction task which is an extension of link prediction in graphs [52]. Our approach is to first learn the features of lower-order simplices and then use an MLP to identify if a simplex is closed or open. We built a SC as [15] on a coauthorship dataset [53] where nodes are authors and collaborations of k -authors are $(k-1)$ -simplices. The input simplicial data is the number of citations, e.g., \mathbf{x}_1 and \mathbf{x}_2 are those of dyadic and triadic collaborations, which does not present explicit properties like forex rates. Thus, 2-simplex (3-simplex) prediction amounts to predict triadic (tetradic) collaborations. From the AUC results in Table 2, we make three observations. 1) SCCNN, MPSN and Bunch [14] methods outperform the rest due to the inter-simplicial couplings. 2) Uncoupling the lower and upper parts in \mathbf{L}_k improves the feature learning (SCNN [19] better than SNN). 3) Higher-order convolution further improves the prediction (SCNN better than PSNN, SCCNN better than Bunch). Note that MPSN has three times more parameters than SCCNN under the settings of the best results.

Ablation study. Table 3 reports the results of SCCNN when certain simplicial relation is missing, which helps understand their roles. When not considering the edge-to-node incidence, it (when using node features) is equivalent to GNN with poor performance. When removing other adjacencies or incidences, the best performance remains but with an increase of model complexity, more layers required. This, however, is not preferred, because the stability decreases as the model deepens and becomes influenced by factors in other simplicial space, as shown in Fig. 1c. We also considered the case with limited input, e.g., when the input on nodes or on edges is missing. The best performance of SCCNN only slightly drops with an increase of convolution order, compared to before $T = 2$.

How tight is the stability bound? We consider the perturbations which relatively shift the eigenvalues of Hodge Laplacians and the singular values of projection matrices by ϵ . We compare the bound in Eq. (5) with experimental distance on each simplex level. Fig. 3 shows the bound becomes tighter as perturbation increases.

Trajectory prediction. We lastly test on predicting trajectories in a synthetic SC and of ocean drifters from [41], introduced by [16]. From Table 4 we first observe SCCNN and Bunch with inter-simplicial couplings do not perform better than those without. This is because zero inputs are applied on nodes and triangles [16], which makes inter-couplings inconsequential. Secondly, using higher-order convolutions improves the

Table 4: Trajectory prediction.

Methods	Synthetic	Ocean drifts
SNN [15]	65.5±2.4	52.5±6.0
PSNN [16]	63.1±3.1	49.0±8.0
SCNN [19]	67.7±1.7	53.0±7.8
Bunch [14]	62.3±4.0	46.0±6.2
SCCNN	65.2±4.1	54.5±7.9

368 average accuracy in both datasets (SCNN better than PSNN on average, SCCNN better than Bunch).
369 Note that the prediction here aims to find a candidate from the neighborhood of end node, which
370 depends on the node degree. Since the average node degree of the synthetic SC is 5.24 and that in
371 ocean drifter data is 4.81, a random guess has around 20% accuracy. The high standard derivations
372 could come from the limited ocean drifter dataset.

373 **Convolution orders on stability.** We also show that NNs with higher-order SCFs have more potential
374 to learn better integral Lipschitz properties, thus, better stability. We consider SCNNs [19] with
375 orders $T_d = T_u = 1, 3, 5$ and train them with a regularizer to reduce the integral Lipschitz constants.
376 As shown in Fig. 4, the higher-order case has a smaller distance (better stability) between the outputs
377 without and with perturbations, with consistent better accuracy, compared to the lower-order case.

378 7 Related Work, Discussion and Conclusion

379 Related work mainly concerns learning methods on SCs. [13] first used $L_{1,d}$ to build NNs on edges in
380 a graph setting without the upper edge adjacency. [15] then generalized convolutional GNNs [32, 51]
381 to simplices by using the Hodge Laplacian. [16, 19] instead uncoupled the lower and upper Laplacians
382 to perform one- and multi-order convolutions, to which [42, 38, 54] added attention schemes. [55]
383 considered a variant of [16] to identify topological holes and [18] combined shifting on nodes and
384 edges for link prediction. Above works learned within a simplicial level and did not consider the
385 incidence relations (inter-simplicial couplings) in SCs, which was included by [14, 20]. These works
386 considered convolutional-type methods, which can be subsumed by SCCNN. Meanwhile, [17, 21]
387 generalized the message passing on graphs [22] to SCs, relying on both adjacencies and incidences.
388 Most of these works focused on extending GNNs to SCs by varying the information propagation
389 on SCs without many theoretical insights into their components. Among them, [16] discussed the
390 equivariance of PSNN to permutation and orientation, which SCCNN admits as well. [17] studied
391 the message-passing on SCs in terms of WL test of SCs built by completing cliques in a graph. The
392 more closely related work [19] gave only a spectral formulation based on SCFs.

393 **Discussion.** In our opinion, the advantage of using SCs is not only about them being able to model
394 higher-order network structure, but also support simplicial data, which can be both human-generated
395 data like coauthorship, and physical data like flow-typed data. This is why we approached the analysis
396 from the perspectives of both simplicial structures and the simplicial data, i.e., the Hodge theory
397 and spectral simplicial theory [23, 9, 26-28, 30, 56]. We provided deeper insights into why three
398 principles are needed and how they can guide the effective and rational learning from simplicial data.
399 As what we practically found, in experiments where data exhibits properties characterized by the
400 Hodge decomposition, SCCNN performs well due to the Hodge-awareness while non-Hodge-aware
401 learners can fail at giving rational results. In cases where data does not possess such properties,
402 SCCNN has better or comparable performance than the ones which violate or do not respect the three
403 principles. This also shows the advantages of SCCNN, especially when data has certain properties.

404 Concurrently, there are works on more general cell complexes, e.g., [57-61], where 2-cells include
405 not only triangles, but also general polygon faces. We focus on SCs because a regular CW complex
406 can be subdivided into a SC [62, 29] to which the analysis in this paper applies, or we can generalize
407 our analysis by allowing B_2 to include 2-cells. This is however informal and does not exploit the
408 power of cell complexes, which lies on cellular sheaves, as studied in [63, 64].

409 **Limitation.** A major limitation of our method is that it cannot learn differently from features at the
410 frequencies of the same type and the same value. For instance, harmonic features are learned in a
411 same fashion because they all have zero frequency. This is however common in convolutional type
412 learning methods on both graphs and SCs. Also, our stability analysis concerns the perturbations on
413 the connection strengths and did not consider the case where simplices join or disappear. Both of
414 them can be interesting future directions, together with more physical-based data applications.

415 **Conclusion.** We proposed three principles for convolutional learning on SCs, summarized in a
416 general architecture, SCCNN. Our analysis showed this architecture, guided by the three principles,
417 demonstrates an awareness of the Hodge decomposition and performs rational, effective and expres-
418 sive learning from simplicial data. Furthermore, our study reveals that SCCNN exhibits stability
419 and robustness against perturbations in the strengths of simplicial connections. Experimental results
420 validate the benefits of respecting the three principles and the Hodge-awareness. Overall, our work
421 establishes a solid foundation for learning on SCs, highlighting the importance of the Hodge theory.

422 **References**

- 423 [1] Mark EJ Newman, Duncan J Watts, and Steven H Strogatz. Random graph models of social networks.
424 *Proceedings of the national academy of sciences*, 99(suppl_1):2566–2572, 2002.
- 425 [2] Austin R Benson, Rediet Abebe, Michael T Schaub, Ali Jadbabaie, and Jon Kleinberg. Simplicial
426 closure and higher-order link prediction. *Proceedings of the National Academy of Sciences*, 115(48):
427 E11221–E11230, 2018.
- 428 [3] Hosein Masoomy, Behrouz Askari, Samin Tajik, Abbas K Rizi, and G Reza Jafari. Topological analysis of
429 interaction patterns in cancer-specific gene regulatory network: persistent homology approach. *Scientific*
430 *Reports*, 11(1):1–11, 2021.
- 431 [4] Federico Battiston, Giulia Cencetti, Iacopo Iacopini, Vito Latora, Maxime Lucas, Alice Patania, Jean-
432 Gabriel Young, and Giovanni Petri. Networks beyond pairwise interactions: structure and dynamics.
433 *Physics Reports*, 874:1–92, 2020.
- 434 [5] Austin R Benson, David F Gleich, and Desmond J Higham. Higher-order network analysis takes off, fueled
435 by classical ideas and new data. *arXiv preprint arXiv:2103.05031*, 2021.
- 436 [6] Leo Torres, Ann S Blevins, Danielle Bassett, and Tina Eliassi-Rad. The why, how, and when of representa-
437 tions for complex systems. *SIAM Review*, 63(3):435–485, 2021.
- 438 [7] Christian Bick, Elizabeth Gross, Heather A Harrington, and Michael T Schaub. What are higher-order
439 networks? *arXiv preprint arXiv:2104.11329*, 2021.
- 440 [8] James R Munkres. *Elements of algebraic topology*. CRC press, 2018.
- 441 [9] Lek-Heng Lim. Hodge laplacians on graphs. *SIAM Review*, 62(3):685–715, 2020.
- 442 [10] Rohan Money, Joshin Krishnan, Baltasar Beferull-Lozano, and Elvin Isufi. Online edge flow imputation
443 on networks. *IEEE Signal Processing Letters*, 2022.
- 444 [11] Junteng Jia, Michael T Schaub, Santiago Segarra, and Austin R Benson. Graph-based semi-supervised &
445 active learning for edge flows. In *Proceedings of the 25th ACM SIGKDD International Conference on*
446 *Knowledge Discovery & Data Mining*, pages 761–771, 2019.
- 447 [12] D Vijay Anand, Soumya Das, and Moo K Chung. Hodge-decomposition of brain networks. *arXiv preprint*
448 *arXiv:2211.10542*, 2022.
- 449 [13] T Mitchell Roddenberry and Santiago Segarra. Hodgenet: Graph neural networks for edge data. In *2019*
450 *53rd Asilomar Conference on Signals, Systems, and Computers*, pages 220–224. IEEE, 2019.
- 451 [14] Eric Bunch, Qian You, Glenn Fung, and Vikas Singh. Simplicial 2-complex convolutional neural networks.
452 In *TDA & Beyond*, 2020. URL <https://openreview.net/forum?id=TLbnsKrt6J->
- 453 [15] Stefania Ebli, Michaël Defferrard, and Gard Spreemann. Simplicial neural networks. In *NeurIPS 2020*
454 *Workshop on Topological Data Analysis and Beyond*, 2020.
- 455 [16] T Mitchell Roddenberry, Nicholas Glaze, and Santiago Segarra. Principled simplicial neural networks for
456 trajectory prediction. In *International Conference on Machine Learning*, pages 9020–9029. PMLR, 2021.
- 457 [17] Cristian Bodnar, Fabrizio Frasca, Yuguang Wang, Nina Otter, Guido F Montufar, Pietro Lio, and Michael
458 Bronstein. Weisfeiler and lehman go topological: Message passing simplicial networks. In *International*
459 *Conference on Machine Learning*, pages 1026–1037. PMLR, 2021.
- 460 [18] Yuzhou Chen, Yulia R. Gel, and H. Vincent Poor. Bscnets: Block simplicial complex neural networks.
461 *Proceedings of the AAAI Conference on Artificial Intelligence*, 36(6):6333–6341, 2022. doi: 10.1609/aaai.
462 v36i6.20583. URL <https://ojs.aaai.org/index.php/AAAI/article/view/20583>
- 463 [19] Maosheng Yang, Elvin Isufi, and Geert Leus. Simplicial convolutional neural networks. In *ICASSP*
464 *2022 - 2022 IEEE International Conference on Acoustics, Speech and Signal Processing (ICASSP)*, pages
465 8847–8851, 2022. doi: 10.1109/ICASSP43922.2022.9746017.
- 466 [20] Ruo Chen Yang, Frederic Sala, and Paul Bogdan. Efficient representation learning for higher-order data with
467 simplicial complexes. In *The First Learning on Graphs Conference*, 2022. URL [https://openreview](https://openreview.net/forum?id=nGqJY4DODN)
468 [net/forum?id=nGqJY4DODN](https://openreview.net/forum?id=nGqJY4DODN)
- 469 [21] Mustafa Hajij, Ghada Zamzmi, Theodore Papamarkou, Vasileios Maroulas, and Xuanting Cai. Simplicial
470 complex representation learning. *arXiv preprint arXiv:2103.04046*, 2021.

- 471 [22] Keyulu Xu, Weihua Hu, Jure Leskovec, and Stefanie Jegelka. How powerful are graph neural networks?
472 *arXiv preprint arXiv:1810.00826*, 2018.
- 473 [23] William Vallance Douglas Hodge. *The theory and applications of harmonic integrals*. CUP Archive, 1989.
- 474 [24] Xiaoye Jiang, Lek-Heng Lim, Yuan Yao, and Yinyu Ye. Statistical ranking and combinatorial hodge theory.
475 *Mathematical Programming*, 127(1):203–244, 2011.
- 476 [25] Ozan Candogan, Ishai Menache, Asuman Ozdaglar, and Pablo A Parrilo. Flows and decompositions of
477 games: Harmonic and potential games. *Mathematics of Operations Research*, 36(3):474–503, 2011.
- 478 [26] Maosheng Yang, Elvin Isufi, Michael T. Schaub, and Geert Leus. Finite Impulse Response Filters
479 for Simplicial Complexes. In *2021 29th European Signal Processing Conference (EUSIPCO)*, pages
480 2005–2009, August 2021. doi: 10.23919/EUSIPCO54536.2021.9616185. ISSN: 2076-1465.
- 481 [27] Sergio Barbarossa and Stefania Sardellitti. Topological signal processing over simplicial complexes. *IEEE*
482 *Transactions on Signal Processing*, 68:2992–3007, 2020.
- 483 [28] John Steenbergen. *Towards a spectral theory for simplicial complexes*. PhD thesis, Duke University, 2013.
- 484 [29] Leo J Grady and Jonathan R Polimeni. *Discrete calculus: Applied analysis on graphs for computational*
485 *science*, volume 3. Springer, 2010.
- 486 [30] Maosheng Yang, Elvin Isufi, Michael T. Schaub, and Geert Leus. Simplicial convolutional filters. *IEEE*
487 *Transactions on Signal Processing*, 70:4633–4648, 2022. doi: 10.1109/TSP.2022.3207045.
- 488 [31] Michael T Schaub, Yu Zhu, Jean-Baptiste Seby, T Mitchell Roddenberry, and Santiago Segarra. Signal
489 processing on higher-order networks: Livin’ on the edge... and beyond. *Signal Processing*, 187:108149,
490 2021.
- 491 [32] Thomas N. Kipf and Max Welling. Semi-supervised classification with graph convolutional networks. In
492 *International Conference on Learning Representations (ICLR)*, 2017.
- 493 [33] Chen Cai and Yusu Wang. A note on over-smoothing for graph neural networks. *arXiv preprint*
494 *arXiv:2006.13318*, 2020.
- 495 [34] T Konstantin Rusch, Michael M Bronstein, and Siddhartha Mishra. A survey on oversmoothing in graph
496 neural networks. *arXiv preprint arXiv:2303.10993*, 2023.
- 497 [35] Hoang Nt and Takanori Maehara. Revisiting graph neural networks: All we have is low-pass filters. *arXiv*
498 *preprint arXiv:1905.09550*, 2019.
- 499 [36] Cameron Ziegler, Per Sebastian Skardal, Haimonti Dutta, and Dane Taylor. Balanced hodge laplacians
500 optimize consensus dynamics over simplicial complexes. *Chaos: An Interdisciplinary Journal of Nonlinear*
501 *Science*, 32(2):023128, 2022.
- 502 [37] Roger A Horn and Charles R Johnson. *Matrix analysis*. Cambridge university press, 2012.
- 503 [38] Lorenzo Giusti, Claudio Battiloro, Paolo Di Lorenzo, Stefania Sardellitti, and Sergio Barbarossa. Simplicial
504 attention networks. *arXiv preprint arXiv:2203.07485*, 2022.
- 505 [39] Danijela Horak and Jürgen Jost. Spectra of combinatorial laplace operators on simplicial complexes.
506 *Advances in Mathematics*, 244:303–336, 2013.
- 507 [40] Nicola Guglielmi, Anton Savostianov, and Francesco Tudisco. Quantifying the structural stability of
508 simplicial homology. *arXiv preprint arXiv:2301.03627*, 2023.
- 509 [41] Michael T Schaub, Austin R Benson, Paul Horn, Gabor Lippner, and Ali Jadbabaie. Random walks on
510 simplicial complexes and the normalized hodge 1-laplacian. *SIAM Review*, 62(2):353–391, 2020.
- 511 [42] Christopher Wei Jin Goh, Cristian Bodnar, and Pietro Lio. Simplicial attention networks. In *ICLR 2022*
512 *Workshop on Geometrical and Topological Representation Learning*, 2022.
- 513 [43] Joan Bruna and Stéphane Mallat. Invariant scattering convolution networks. *IEEE transactions on pattern*
514 *analysis and machine intelligence*, 35(8):1872–1886, 2013.
- 515 [44] Qiang Qiu, Xiuyuan Cheng, Guillermo Sapiro, et al. Dcfnet: Deep neural network with decomposed
516 convolutional filters. In *International Conference on Machine Learning*, pages 4198–4207. PMLR, 2018.

- 517 [45] Alberto Bietti and Julien Mairal. Group invariance, stability to deformations, and complexity of deep
518 convolutional representations. *arXiv preprint arXiv:1706.03078*, 2017.
- 519 [46] Fernando Gama, Alejandro Ribeiro, and Joan Bruna. Stability of graph scattering transforms. *Advances in*
520 *Neural Information Processing Systems*, 32, 2019.
- 521 [47] Fernando Gama, Joan Bruna, and Alejandro Ribeiro. Stability properties of graph neural networks. *IEEE*
522 *Transactions on Signal Processing*, 68:5680–5695, 2020.
- 523 [48] Henry Kenlay, Dorina Thano, and Xiaowen Dong. On the stability of graph convolutional neural networks
524 under edge rewiring. In *ICASSP 2021-2021 IEEE International Conference on Acoustics, Speech and*
525 *Signal Processing (ICASSP)*, pages 8513–8517. IEEE, 2021.
- 526 [49] Alejandro Parada-Mayorga, Zhiyang Wang, Fernando Gama, and Alejandro Ribeiro. Stability of aggrega-
527 tion graph neural networks. *arXiv preprint arXiv:2207.03678*, 2022.
- 528 [50] Oanda Corporation. Foreign exchange data. <https://www.oanda.com/>, 2018/10/05.
- 529 [51] Michaël Defferrard, Xavier Bresson, and Pierre Vandergheynst. Convolutional neural net-
530 works on graphs with fast localized spectral filtering. In D. Lee, M. Sugiyama, U. Luxburg,
531 I. Guyon, and R. Garnett, editors, *Advances in Neural Information Processing Systems*, volume 29.
532 Curran Associates, Inc., 2016. URL [https://proceedings.neurips.cc/paper/2016/file/](https://proceedings.neurips.cc/paper/2016/file/04df4d434d481c5bb723be1b6df1ee65-Paper.pdf)
533 [04df4d434d481c5bb723be1b6df1ee65-Paper.pdf](https://proceedings.neurips.cc/paper/2016/file/04df4d434d481c5bb723be1b6df1ee65-Paper.pdf).
- 534 [52] Muhan Zhang and Yixin Chen. Link prediction based on graph neural networks. *Advances in neural*
535 *information processing systems*, 31, 2018.
- 536 [53] Waleed Ammar, Dirk Groeneveld, Chandra Bhagavatula, Iz Beltagy, Miles Crawford, Doug Downey, Jason
537 Dunkelberger, Ahmed Elgohary, Sergey Feldman, Vu Ha, et al. Construction of the literature graph in
538 semantic scholar. *arXiv preprint arXiv:1805.02262*, 2018.
- 539 [54] See Hian Lee, Feng Ji, and Wee Peng Tay. Sgat: Simplicial graph attention network. *arXiv preprint*
540 *arXiv:2207.11761*, 2022.
- 541 [55] Alexandros D Keros, Vidit Nanda, and Kartic Subr. Dist2cycle: A simplicial neural network for homology
542 localization. *Proceedings of the AAAI Conference on Artificial Intelligence*, 36(7):7133–7142, 2022. doi:
543 10.1609/aaai.v36i7.20673. URL <https://ojs.aaai.org/index.php/AAAI/article/view/20673>.
- 544 [56] Kiya W Govek, Venkata S Yamajala, and Pablo G Camara. Spectral simplicial theory for feature selection
545 and applications to genomics. *arXiv preprint arXiv:1811.03377*, 2018.
- 546 [57] Mustafa Hajij, Kyle Istvan, and Ghada Zamzmi. Cell complex neural networks. In *NeurIPS 2020 Workshop*
547 *on Topological Data Analysis and Beyond*, 2020.
- 548 [58] Mustafa Hajij, Ghada Zamzmi, Theodore Papamarkou, Nina Miolane, Aldo Guzmán-Sáenz, and
549 Karthikeyan Natesan Ramamurthy. Higher-order attention networks. *arXiv preprint arXiv:2206.00606*,
550 2022.
- 551 [59] Stefania Sardellitti, Sergio Barbarossa, and Lucia Testa. Topological signal processing over cell complexes.
552 In *2021 55th Asilomar Conference on Signals, Systems, and Computers*, pages 1558–1562. IEEE, 2021.
- 553 [60] T Mitchell Roddenberry, Michael T Schaub, and Mustafa Hajij. Signal processing on cell complexes. In
554 *ICASSP 2022-2022 IEEE International Conference on Acoustics, Speech and Signal Processing (ICASSP)*,
555 pages 8852–8856. IEEE, 2022.
- 556 [61] Cristian Bodnar, Fabrizio Frasca, Nina Otter, Yu Guang Wang, Pietro Liò, Guido F Montufar, and Michael
557 Bronstein. Weisfeiler and lehrman go cellular: Cw networks. *Advances in Neural Information Processing*
558 *Systems*, 34, 2021.
- 559 [62] Albert T Lundell, Stephen Weingram, Albert T Lundell, and Stephen Weingram. Regular and semisimplicial
560 cw complexes. *The Topology of CW Complexes*, pages 77–115, 1969.
- 561 [63] Jakob Hansen and Robert Ghrist. Toward a spectral theory of cellular sheaves. *Journal of Applied and*
562 *Computational Topology*, 3(4):315–358, 2019.
- 563 [64] Cristian Bodnar, Francesco Di Giovanni, Benjamin Chamberlain, Pietro Liò, and Michael Bronstein.
564 Neural sheaf diffusion: A topological perspective on heterophily and oversmoothing in gnns. *Advances in*
565 *Neural Information Processing Systems*, 35:18527–18541, 2022.
- 566 [65] Elvin Isufi and Maosheng Yang. Convolutional filtering in simplicial complexes. In *ICASSP 2022 - 2022*
567 *IEEE International Conference on Acoustics, Speech and Signal Processing (ICASSP)*, pages 5578–5582,
568 2022. doi: 10.1109/ICASSP43922.2022.9746349.